ISSN 1027-5495. Functional Materials, 33, No.1 (2026), p. 61-69
doi:http://dx.doi.org/10.15407/fm33.01.61

Surface modification of the cobalt base super alloy using titanium oxide as thermal barrier and study of its efficiency in resisting oxidation and hot corrosion

Kheder A. Salah*, Mazin A. Abed, Mahmood A. Hamood

Department of Physics, College of Science, University of Mosul, Iraq
* khederali@uomosul.edu.iq

Received April 9, 2025 approved 14.01.2026

In this study, the efficiency of the improved super alloy on cobalt base (F-75) by modifying the surface components of the alloy using the diffusion coating method in aluminum with presence of the thermal barrier of titanium oxide (TiO_2)at 1070 ° C and in a vacuum atmosphere to avoid oxidation. The periodic oxidation process and a hot corrosion process was performed on the samples at a temperature of (1100°C) with the presence of sodium sulfate (Na_2SO_4) and sodium chloride (NaCl), to determine their behavior on the one hand, and to study the structural composition of the samples through a set of technical tests, including optical microscopy,x-ray diffraction (XRD(, scanning electron microscope (SEM) as well as quantitative and qualitative examinations through the energy dispersive spectroscopy (EDS), specifications for the prepared alloys

Keywords: Diffusion coatings of aluminum, thermal barrier of Titanium oxide (TiO_2) ,super alloy cobalt base F-75,oxidation and hot corrosion

Модифікація поверхні суперсплаву на основі кобальту з використанням оксиду титану як теплового бар'єру та дослідження його ефективності в опорі окисленню та гарячій корозії. *Kheder A. Salah, Mazin A. Abed, Mahmood A. Hamood*

Досліджується ефективність покращеного суперсплаву на основі кобальту (F-75) шляхом модифікації поверхневих компонентів сплаву за допомогою методу дифузійного покриття в алюмінії з присутністю теплового бар'єру з оксиду титану (TiO_2) при 1070 °C та у вакуумній атмосфері для запобігання окисленню. Періодичний процес окислення та процес гарячої корозії проводилися на зразках за температури (1100°C) у присутності сульфату натрію (Na_2SO_4) та хлориду натрію (NaCl), щоб визначити їхню поведінку, з одного боку, та вивчити структурний склад зразків за допомогою комплексу технічних випробувань, включаючи оптичну мікроскопію, рентгенівську дифракцію (XRD), скануючий електронний мікроскоп (SEM), а також кількісні та якісні дослідження за допомогою енергодисперсійної спектроскопії (EDS), специфікації для отриманих сплавів.

1. Introduction

The durability of metallic components in high-temperature engines has long been a major concern in both research and industrial practice. Among the most damaging factors are hot corrosion and oxidation, which arise through complex interactions between metallic surfaces and aggressive operating environments. These processes often lead to premature failure of critical components such as turbine blades and combustor liners, thereby limiting engine performance and reliability [1,2]. Hot corrosion typically develops when metals are exposed to reactive salts such as sodium sulfate (Na_2SO_4) and sodium chloride (NaCl) in the presence of oxygen. At elevated tempera-

tures, these compounds accelerate chemical attack and destabilize the protective oxide films that normally shield the alloy [3,4]. Oxidation, though more fundamental in nature, is equally destructive, as the direct reaction of oxygen with the metal surface leads to the formation of oxide scales, depletion of key alloying elements, and eventual material degradation [5,6]. The severity and morphology of such damage are influenced by a range of factors, including the chemical composition of the alloy, the surface condition, the concentration of salts, the velocity of hot gases, and the operating temperature. As a result, corrosion may present in the form of localized pitting, cracking, or grooving, each of which undermines the mechanical integrity of the material [7–9]. To mitigate these effects, thermal Introuction coatings (TBCs) have been developed and widely applied in advanced turbine systems. A conventional TBC comprises a ceramic topcoat deposited over a metallic bond coat, together forming a multilayer system that not only acts as a thermal insulator but also provides resistance against oxidation and hot corrosion. In doing so, TBCs significantly improve the reliability and service life of high-temperature components [10–12]. Within this context, cobalt-based superalloys occupy a particularly important role. Since their development in the early twentieth century, they have been used extensively in gas turbines and jet engines because of their excellent resistance to oxidation and hot corrosion at elevated temperatures. Their superior properties arise from their complex chemistry: chromium (Cr) contributes to the formation of a stable protective oxide (Cr_2O_3), nickel (Ni) improves toughness, molybdenum (Mo) and tungsten (W) increase hardness and strength, while carbon (C), especially when combined with chromium, promotes the formation of carbides that enhance both hardness and wear resistance [13–15]. Compared with nickel-based superalloys, cobalt-based alloys are distinguished by their remarkable thermal stability, maintaining structural integrity during prolonged exposure to extreme temperatures and repeated thermal cycling. This makes them particularly valuable in the rear sections of turbine engines, where environmental degradation dominates. Nickel-based alloys, although less thermally stable, exhibit superior mechanical strength under high stress, which explains their preferential use in the front stages of turbines where mechanical loading is greatest [16–19]. The study of hot corrosion and oxidation in cobalt-based superalloys therefore remains both scientifically relevant and technologically urgent, as advances in engine efficiency and service life depend on a deeper understanding of these degradation mechanisms and the development of improved alloy and coating systems. The aim of this study is to identify and improve the performance of the alloy (F-75) when exposed to harsh conditions such as high temperatures in the presence of a mixture of salts vapors , where oxidation and hot corrosion of the alloy samples were studied when exposed to a vapors of salts mixture (sodium sulfate (Na_2SO_4) and sodium chloride (NaCl)) at 1100°C

2. Experimental

Super alloy cobalt base F-75 samples with dimensions appropriate for the coating system have been prepared table (1). In order to remove the oxide layer from the sample surfaces, silicon carbide papers with 180, 220, 240, 320, 400, 600, 800, 1000, 1200, 1500 and 2000 granular sizes were used.

The samples cleaned using alcohol and distilled water then allowed to dry. Finally, the samples weighed with a sensitive balance before coating process, Some samples were coated with single aluminum by cementation process, where they immersed in a mixture containing different concentrations of aluminum, ammonium chloride (NH_4Cl) and aluminum oxide Al_2O_3 powders as shown in table (2), While titanium oxide (as a thermal barrier coating) was bonded to the other sample surfaces using a local chemical bonding material (super power glue), the samples then immersed in the same mixture to be coated with aluminum.

The cementation process

It was performed on all samples by immersing them completely in a sealed tightly quartz package with the coating mixture, the package then placed in a evacuated closed quartz tube

Table 1. Chemical compositions of Super alloy cobalt base F-75[20]

alloy	C	Mn	Si	Cr	Ni	Mo	W	Fe	Co
F-75	0.25	0.5	0.8	28	<1	6	<0.2	<0.75	Bal.

Table 2. The coating material concentrations in cement powder

material	Percent
aluminum	25%
ammonium chloride (NH_4Cl) powder	5%
Alumina (aluminum oxide Al_2O_3)	70%

(10^{-3}-10^{-2} torr) figure (1). The quartz tube heated in a furnace to 1070°C for different periods (2,4,6, and 8 hr.). finally, The samples left to cool to 25 °C in the furnace, then washed, dried and weighted[12][13].

The Oxidation and hot corrosion processes

The mixture of 12.5g sodium sulfate and 12.5g of sodium chloride were dissolved in 1 liter of distilled water. The solution was heated, and the vapors of these salts were directed onto the samples inside an furnace at 1100 °C figure 2.

Samples were weighed and cleaned after exposure to oxidation and hot corrosion every three hours for 324 hours.

Optical microscope imaging

Imaging of the samples with optical microscope required performing of several processes including

- grinding process using of silicon carbide paper With different roughness ranging from 180 to 2000.
- polishing process using diamond paste or alumina solution (Al_2O_3)
- washing samples by distilled water and alcohol respectively and left to dry.
- Etching by Keller solution (it is a mixture of hydrofluoric acid (0.5%HF), hydrochloric acid (1.5%HCL), nitric acid (2.5%HNO_3) and the rest is distilled water)to show the coating layers structure.

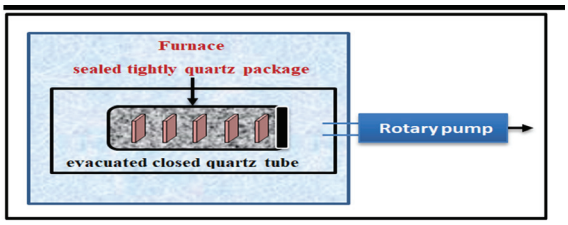

Figure 1. Schematic diagram of the cementation coating system

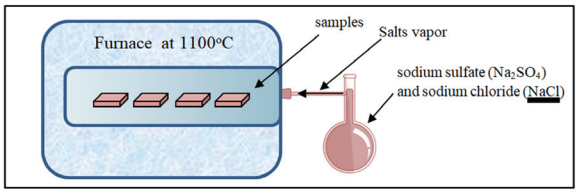

Figure 2. Schematic diagram of Oxidation and hot corrosion system

3. Results And Discussion

The coating process was carried out with titanium oxide (TiO_2) as a thermal barrier coatings (TBC) at 1070°C in vacuum (10^{-3}-10^{-2} tore) and for different periods 2,4,6 and 8 hrs., the microscopic examination images showed a three layers after coating periods 4 and 8 hrs. as shown in figure(3), and these layers are :

- The outer layer can be distinguished by its dark green color and contains a group of phases rich in aluminum, it may be also characterized by the presence of carbide deposits of different colors ,such as light brown , dark brown and light yellow , it may be attacked by the etching solution as shown in figure 3 and figure 4.
- The inner layer (less attacked to the etching solution), it is a thin layer and has light green color and does not contain a deposits.
- Enter diffusion zone, it is a very narrow layer, almost free of deposits, that separates the coating layer from the base

The x-ray diffraction pattern (XRD) of the samples coated by single aluminum for 4 and

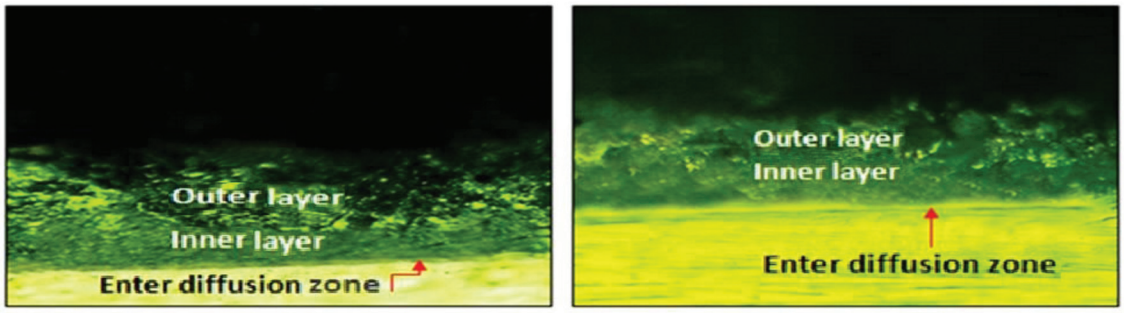

Figure 3. Microscopic composition of single aluminized coating of cobalt base (F-75) at a temperatures 1070 °C for (a-4 hrs., b- 8 hrs.)

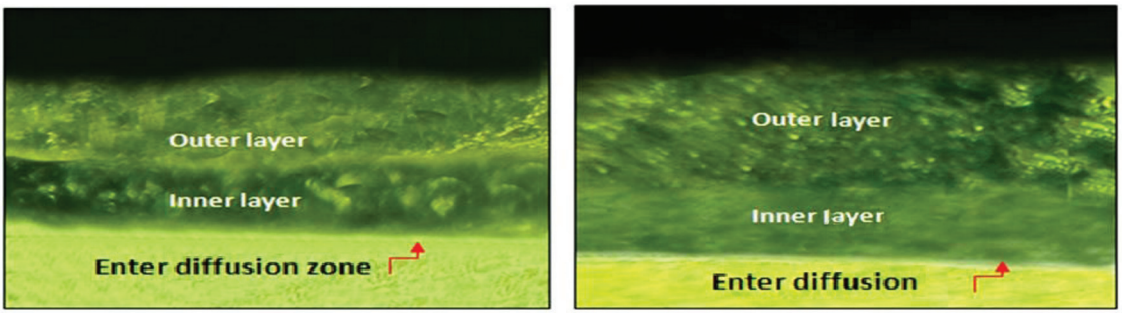

Figure 4. Microscopic composition of thermal barrier coatings (TBC_S) TiO_2 of cobalt base (F-75) at a temperature 1070°C for (a-4hrs. b- 8hrs.)

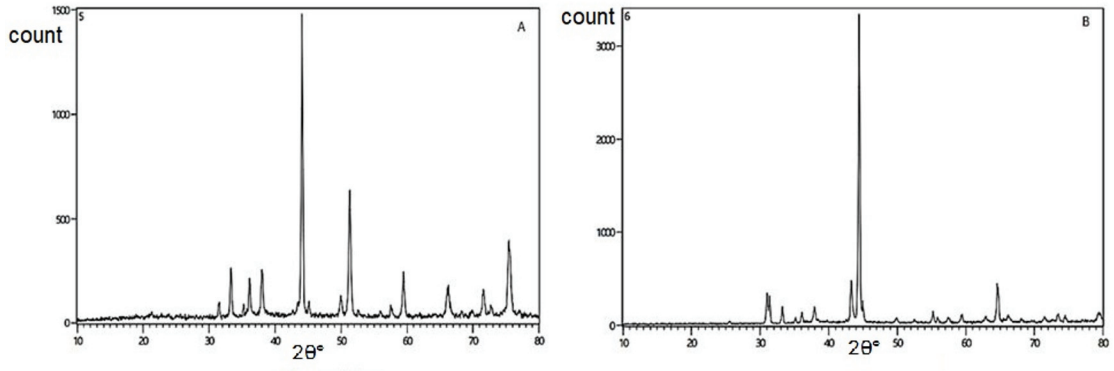

Figure 5. X-ray diffraction (XRD) spectrum indicating the presence of different phases formed in samples coated by single aluminized at 1070 ^{0}C for (a)4 and (b)8 hrs.

8 periods showed in figure (5), the basic stable phase was (CoAl) in addition to another rich aluminum phases including Iron-aluminum (Fe_4Al_{13}), and Chrome -Aluminum ($CrAl_2$) ($CrAl_5$) phases figure (5).

The x ray spectrum of the samples coated by aluminum with the presence of thermal barrier shown in figure (6), they do not differ much from those that coated with single aluminum, the phase (CoAl) was the most stable phase in addition to $CoAl_3$, Co_2Al_3 and CoAl phases. The secondary phases including Iron-Aluminum (Fe_4Al_{13}) , chromium compounds-aluminum phases ($CrAl_2$,$CrAl_3$, CrAl) and titanium phases $TiAl_3$, Ti_3Al_5 , Al_3Ti ,Al_2Ti Al_3Ti_2 and TiO_2 [21][22].

The energy dispersive spectrum (EDS) show the variation of the aluminum concentration

Table 3. The quantitative and qualitative ratios of the super alloy cobalt base F-75 coating with a single aluminum and aluminum with presence of thermal barrier (titanium oxide) for 4 and 8hrs. at 1070 °C

Elt	Al – 4hrs.		Al-8hrs.		Al+TiO_2-4hrs		Al+TiO_2-8hrs	
	W%	A%	W%	A%	W%	A%	W%	A%
C	17.89	27.14	12.53	17.93	4.17	9.39	-	-
Ni	16.43	21.38	19.85	24.37	19.19	37.02	-	-
O	27.57	31.39	38.73	41.61	8.68	14.66	25.78	38.79
Al	19.83	13.39	19.90	12.68	1.17	1.18	1.27	1.39
S	3.72	2.11	2.30	1.23	5.51	4.65	13.59	10.20
Co	5.50	2.50	2.31	0.99	0.44	0.30	10.56	6.34
Ti	-	-	-	-	26.84	15.14	48.8	43.28
Cr	1.93	0.68	2.55	0.84	34.00	17.67	-	-
Fe	0.38	0.12	0.17	0.05	-	-	-	-
Mo	6.75	1.28	1.67	0.30	-	-	-	-
	100.00	100.00	100.00	100.00	100.00	100.00	100.00	100.00

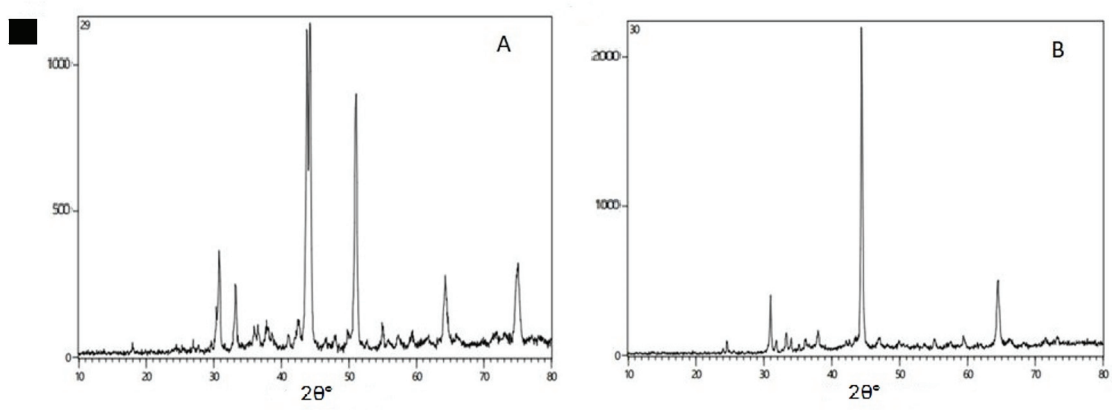

Figure 6 X-ray diffraction (XRD) spectrum indicating the presence of different phase formed in samples coated with aluminized with presence of thermal barrier oxide (TiO_2) at 1070 ^{0}C for(a)4 and(b) 8 hrs.

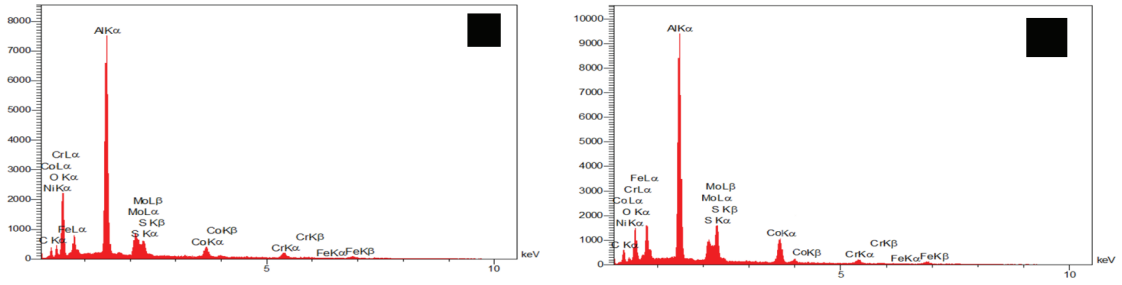

Figure 7. Energy dispersive spectroscopy (EDS) for a single aluminizing coating at (a- 4 hrs. , b- 8 hrs.) on a super alloy cobalt base F-75 at temperature 1070 ^{0}C

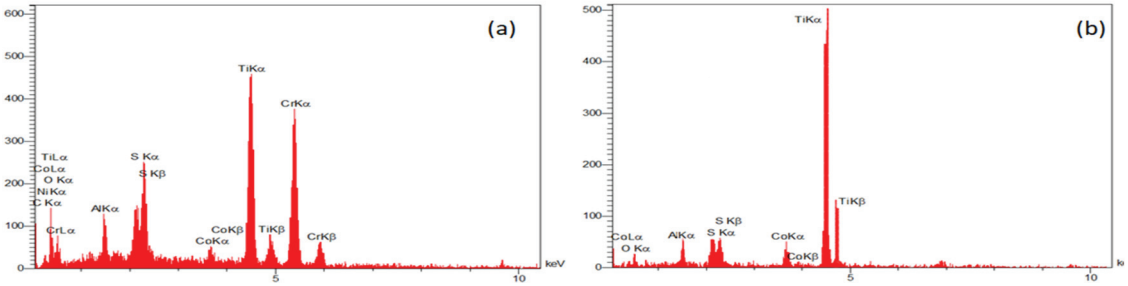

Figure 8. Energy dispersive spectroscopy (EDS) for aluminizing coating with presence a thermal barrier oxide coating (TBC) of (TiO_2) on a super alloy cobalt base F-75 at temperature 1070 ^{0}C

in the samples coated by single aluminum and samples coated by aluminum with presence of thermal barrier coating figure(7) and figure(8) respectively . The aluminum concentration increase in the samples coated by aluminum with presence of titanium oxide as thermal barrier because of the presence of the most quantity of aluminum on the alloy surface as a result of the thermal barrier impeding the aluminum diffusion into the depth of the alloy, in addition to impeding the diffusion of the alloy's elements outward Table 1 and Table 2.

The aluminum and oxygen elements increase in the alloy with coating period of single aluminum ,while carbon concentration decrease Table 1, but for the samples coated by aluminum with the presence of titanium oxide as a thermal barrier, the aluminum and oxygen concentration increases with coating time Table 1, which is an important point in the super alloy surface modification and surface engineering process, it means that the casting elements quantity in the original super alloy can be controlled according to the specifications needed by the research.

The scanning electron microscope images show the variation of the structure in all samples figure(9), the images of the samples coated by single aluminum show an decrease in the grain dimensions with coating periods as a re-

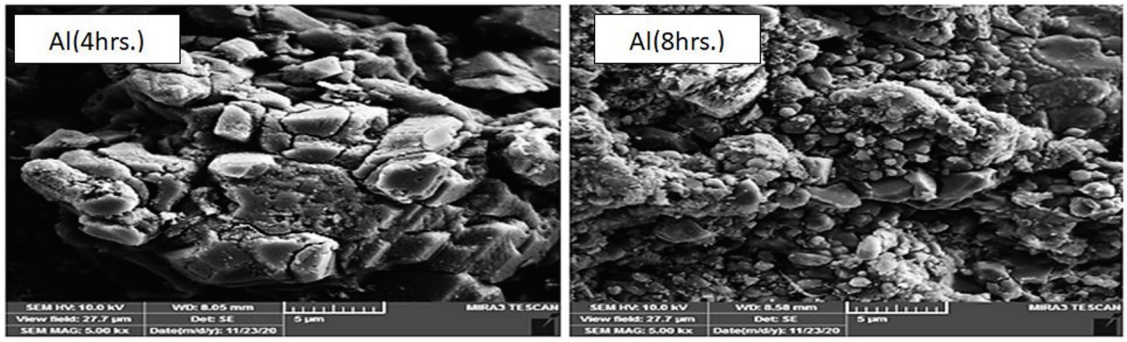

Figure 9. Scanning electron microscopy (SEM) for a single aluminizing coating at (a-4 hrs. , b- 8 hrs.)on a super alloy cobalt base F-75 at temperature 1070 ^{0}C

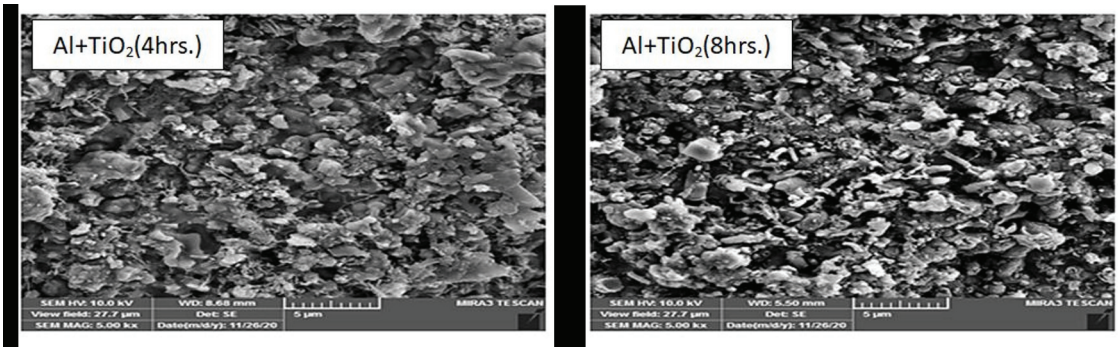

Figure 10. Scanning electron microscopy (SEM) for aluminizing coating with presence a thermal barrier coating (TBC) of titanium oxide (TiO_2) at (a- 4 hrs. , b- 8 hrs.) on a super alloy cobalt base F-75 at temperature 1070 ^{0}C.

sult of the recrystallization process and this is accompanied by an increase in the diffusion of the aluminum element within the alloy over time, while the samples coated with aluminum with presence of thermal barrier images show the porosity of the thermal barrier which Obstructed the diffusion process through the barrier in both sides figure (10).

in the aggregation of the grains , while the samples that treated for 4 hrs. show the formation of linear structures with Nano diameters and the increase of the treating to 8 hrs. will increase the growth and aggregation figure(8).

The weight gain as mean (up take) was calculated during the alumnization of pack cementation process, it is increases with time according to the shape of the parabola figure (11) and table (3). The weight gained increases with coating time also according to the shape of the parabola because the weight gained is governed by the diffusion processes which is in turn governed by the parabola shape.

In another aspect, the coating thickness increases with coatings time for single aluminization coating and aluminization with presence of thermal barrier coating (TBC). We notice through figure 14.That the amount of weight gained in single aluminize coating is greater than the aluminum coating with presence of the thermal barrier oxide because the thermal

Table 3. average weight gain for super alloy cobalt base F-75 of single aluminize coating, and aluminized coating with presence of thermal barrier coating (TBC) of titanium oxide (TiO_2)

Temperature °C	Coating Temp.(hr)	Average weight gain of single aluminize coating (gm/cm^2)	Average weight gain of aluminized coating with presence of (TBC) (gm/cm^2)
1070	0	0	0
	2	0.115	0.0907
	4	0.21	0.142
	6	0.2582	0.19265
	8	0.261	0.202

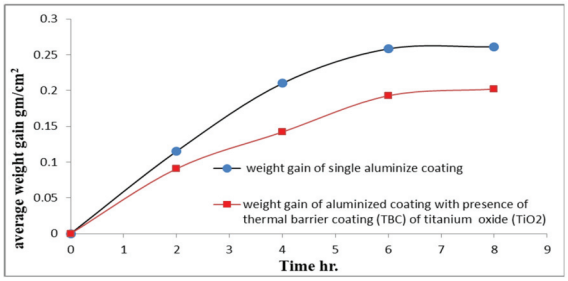

Figure 11 Weight gain of the super alloy of cobalt base F-75 coating at 1070 °C as a function of time for (a)single aluminize coating, (b) aluminized coating with presence of thermal barrier coating (TBC) of titanium oxide (TiO2).

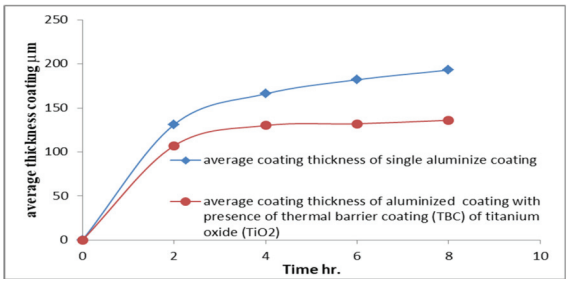

Figure 12. The thickness of the super alloy of cobalt base F-75 coating at 1070 °C as a function of time for (a) single aluminize coating, and (b) aluminized coating with presence of thermal barrier coating (TBC) of titanium oxide (TiO_2)

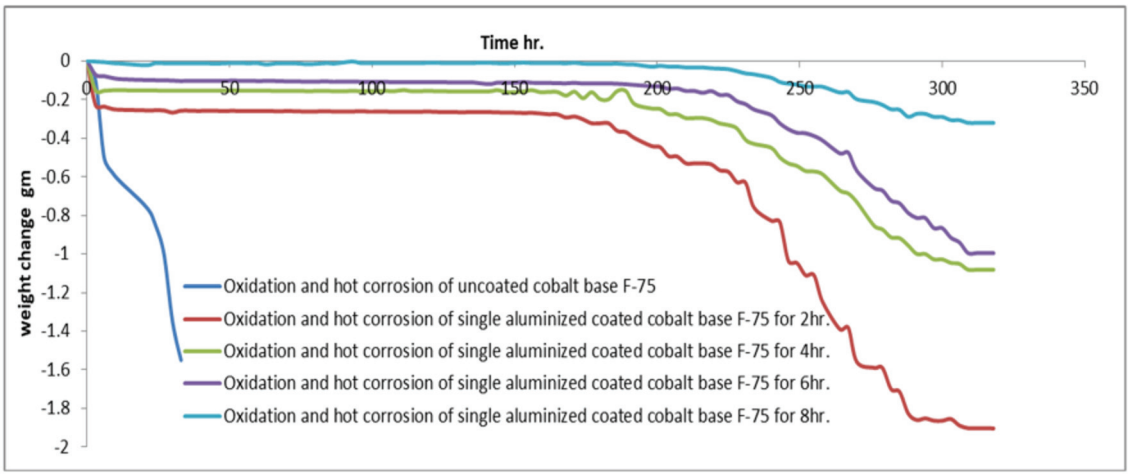

Figure 13. Cycle oxidation and hot corrosion of single aluminized coatings of super alloy cobalt base F-75 by exposure to a mixture of salt vapor Na_2SO_4 and NaCl for 325hrs.(3hrs. cycle) in atmosphere at 1100 ^{0}C .

barrier oxide reduced the weight gained during the aluminization due to the porosity of the thermal barrier which Impedes the diffusion of the elements through it in both sides .

The periodic of oxidation and hot corrosion of the coated samples by single aluminum are depicted in figure (12) , as they exposed for 325hrs. at 1100°C to a vapor of a mixture of sodium chloride (NaCl) and sodium sulfate (Na_2SO_4) for three hours per cycle , almost all samples show a stability in weight with time, noting that the samples that coated for 6 and 8 hrs. were more stable in weight with time than the samples that coated for 2 and 4 hrs. , the decrease in weight is due to the formation of unstable oxide (θ-Al_2O_3) before the for-

Table 4. Average coating thickness for super alloy cobalt base F-75 of single aluminize coating, and aluminized coating with presence of thermal barrier coating (TBC) of titanium oxide (TiO_2)

Temperature °C	Coating Temp.(hr)	Average thickness of single aluminize coating (µm)				Average thickness of aluminized coating with presence of (TBC) of titanium oxide (TiO_2) (µm)			
		Outer layer	Inner layer	Inter diffusion zone	Total	Outer layer	Inner layer	Inter diffusion zone	Total
	0	0	0	0	0	0	0	0	0
1070	2	58	42	31	131	48	26	33	107
	4	68	52	46	166	61	33	36	130
	6	76	54	52	182	68	37	27	132
	8	89	61	43	193	73	29	34	136

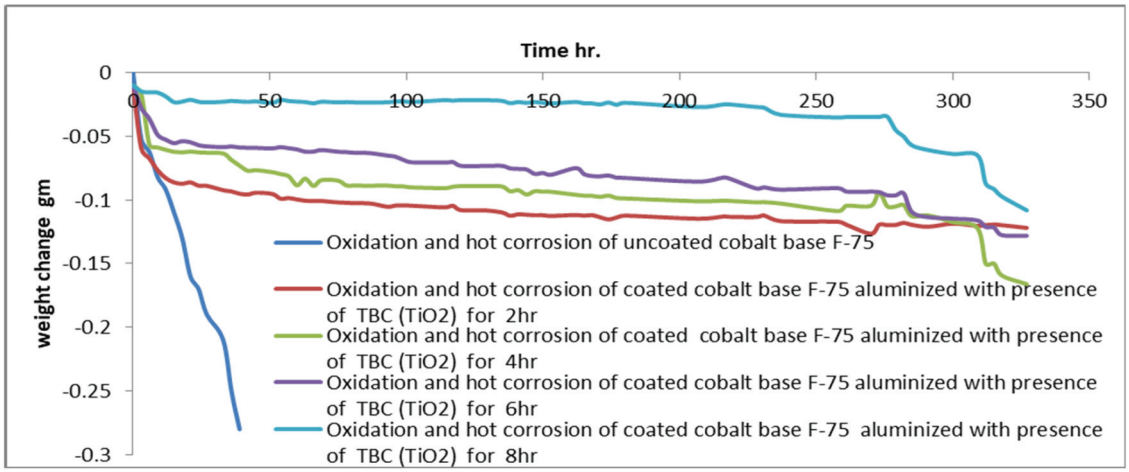

Figure 14.Cycle oxidation and hot corrosion of the aluminum coating of super alloy cobalt base F-75 in the presence of a thermal barrier titanium oxide (TiO_2) by exposure to a mixture of salt vapor Na_2OS_4 and NaCl for 325hrs.(3hrs. cycle) in atmosphere at 1100 ^{0}C.

mation of stable protective oxide (α-Al_2O_3). It is worth mentioning that at a temperatures above 900 °C, the volatile compounds CrO_3 was produced from the protective oxide scale, Cr_2O_3[23].

The same response was observed for the samples coated by aluminum in the presence of thermal barrier coating (TiO_2), but the main difference was the decrease in weight change in comparison to the samples coated with single aluminum over the total exposure time (325hrs) as in figure(14), this decrease was due to the presence of thermal barrier which obstructs the spread of the elements through it.

4. Conclusions

Group of samples were prepared from super alloy cobalt base F-75 , some of these samples were coated by single aluminum and the rest were coated by aluminum with presence of thermal barrier oxide titanium oxide (TiO_2). The x ray diffraction pattern (XRD) of the samples coated for 4 and 8 periods by single aluminum and aluminum with the presence of thermal barrier showed the presence of basic stable phase (CoAl) in addition to another rich aluminum phases (Co_2Al_3)(Co Al_3) ,Chromium-Aluminum phases ($CrAl_2$,$CrAl_3$, CrAl) , Iron-aluminum (Fe_4Al_{13}) phase and titanium phases $TiAl_3$, Ti_3Al_5 , Al_3Ti ,Al_2Ti Al_3Ti_2 and TiO_2. The scanning electron microscope images show an increase in the aggregation of the grains. The weight gain increases with time according to the shape of the parabola, the amount of weight gained in single aluminize coating is greater than the aluminum coating with presence of the thermal barrier oxide. Finally , The oxidation and hot corrosion of the samples coated by single aluminum have more stability in weight with time than the samples that coated by aluminized with presence of the thermal barrier. The alumina oxide protection scale (Al_2O_3) that adhere to the alloy surface strongly will prevent the alloy from the high tempertures.

References

1. Pettit, F. (2011). Hot corrosion of metals and alloys. Oxidation of Metals, 76, 1-21.
2. Rosso, M., Peter, I., & Gobber, F. S. (2015). Overview of heat treatment and surface engineering, influences of surface finishing on hot–work tool steel. International Journal of Microstructure and Materials Properties, 10(1), 3-30.
3. Sidhu, T. S., Prakash, S., & Agrawal, R. D. (2006). Hot corrosion and performance of nickel-based coatings. Current science, 41-47.
4. Shifler, D. A. (2003). High-temperature gaseous corrosion testing.
5. Asri, R. I. M., Harun, W. S. W., Samykano, M., Lah, N. A. C., Ghani, S. A. C., Tarlochan, F., & Raza, M. R. (2017). Corrosion and surface modification on biocompatible metals: A review. Materials Science and Engineering: C, 77, 1261-1274.
6. Shreir, L. L. (Ed.). (2013). Corrosion: metal/environment reactions. Newnes.
7. Ahmad, Z. (2006). Principles of corrosion engineering and corrosion control. Elsevier.
8. Roberge, P. R., & Eng, P. (2005). Corrosion engineering. Principles and Practice, 1.
9. McCafferty, E. (2010). Introduction to corrosion science. Springer Science & Business Media.

10. Kumar, V., & Balasubramanian, K. (2016). Progress update on failure mechanisms of advanced thermal barrier coatings: A review. Progress in Organic Coatings, 90, 54-82.
11. Thakare, J. G., Pandey, C., Mahapatra, M. M., & Mulik, R. S. (2021). Thermal barrier coatings—A state of the art review. Metals and Materials International, 27, 1947-1968.
12. Wang, L., Li, D. C., Yang, J. S., Shao, F., Zhong, X. H., Zhao, H. Y., ... & Wang, Y. (2016). Modeling of thermal properties and failure of thermal barrier coatings with the use of finite element methods: A review. Journal of the European Ceramic Society, 36(6), 1313-1331.
13. Marti, A. (2000). Cobalt-base alloys used in bone surgery. Injury, 31, D18-D21.
14. Schilke, P. W. (2004). Advanced gas turbine materials and coatings. GE Energy.
15. Pilliar, R., & Ramsay, S. D. (2012). Cobalt-base alloys.
16. Sato, J., Omori, T., Oikawa, K., Ohnuma, I., Kainuma, R., & Ishida, K. (2006). Cobalt-base high-temperature alloys. Science, 312(5770), 90-91.
17. Mohapatra, J., Xing, M., Elkins, J., & Liu, J. P. (2020). Hard and semi-hard magnetic materials based on cobalt and cobalt alloys. *Journal of Alloys and Compounds*, *824*, 153874.
18. Crook, P. (1990). Cobalt and cobalt alloys.
19. Armyanov, S. (2000). Crystallographic structure and magnetic properties of electrodeposited cobalt and cobalt alloys. Electrochimica Acta, 45(20), 3323-3335.
20. Akca, E., & Gürsel, A. (2015). A review on superalloys and IN718 nickel-based INCONEL superalloy. Periodicals of engineering and natural sciences, 3(1).
21. Wang, P. Y., Li, H. J., Qi, L. H., Zeng, X. H., & Zuo, H. S. (2011). Synthesis of Al-TiAl3 compound by reactive deposition of molten Al droplets and Ti powders. Progress in Natural Science: Materials International, 21(2), 153-158.
22. Yan, Z., XinLei, Z., WenBao, J., Qing, S., YongSheng, L., DaQian, H., & Da, C. (2016). Online X-ray fluorescence (XRF) analysis of heavy metals in pulverized coal on a conveyor belt. Applied spectroscopy, 70(2), 272-278.